

GA Based Optimal Design of Shaded Pole Motor

V.Sarac, L.Petkovska, M.Cundev and G.Cvetkovski

Ss. Cyril and Methodius University, Faculty of Electrical Engineering phone: (+389) 2 3099 145, fax: (+389) 2 3064 262,

e-mail: vasilija.sarac@siemens.com.mk; lidijap@etf.ukim.edu.mk

Abstract — Method of Genetic Algorithms-GA is applied in order to create optimised model of shaded pole motor-SPM starting from prototype. Optimisation is achieved by developing model with greater electromagnetic torque, weaker flux density and improved dynamic characteristics. Prototype and GA optimised model are analysed using equivalent circuit method -ECM, Finite Element Method – FEM and MATLAB/SIMULINK-MSM.

I. INTRODUCTION

In the engineering practice, a concept of optimization means creating better and more economical solution by using existing resources. This point of view is especially important in the design of electrical machines.

The paper presents an extension of authors' previous works related to GA application as a powerful tool for optimization of electrical machines, and in particular of a shaded pole motor [1]. New optimal model will be derived by using electromagnetic torque as target function, but with less constraints in the motor cross section geometry. The torque at rated slip in the new optimal model will be greater, and the efficiency will be improved. Afterwards, a deepened analysis of shaded pole motor models will be performed by using Finite Element Method for magnetic field calculations and MATLAB/SIMULINK for prediction of their dynamic behaviour.

II. MOTOR DESCRIPTION

As an object of investigation a single phase shaded pole motor type AKO-16, product of "Mikron", is considered. The rated motor data are as follows: $U_n=220\text{ V}$; $f_n=50\text{ Hz}$; $I_n=0.125\text{ A}$; $2p=2$; $P_1=18\text{ W}$; $n_n=2520\text{ rpm}$. This motor is adopted as a prototype – *basic model*. In order to improve its performance characteristics, an optimization procedure, based on GA is carried out. The optimization variables are: current density, magnetic flux density, core length, stator pole width, pole shading portion and angle of rotor skew consequently, all windings' parameters will be changed.

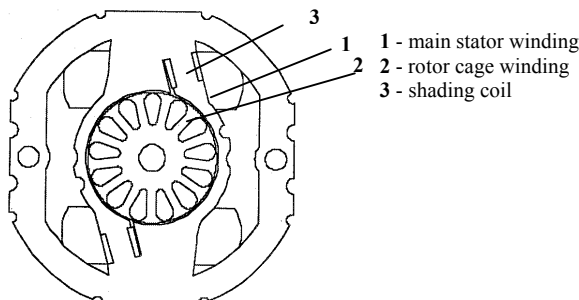


Figure 1. Motor cross-section

III. METHOD OF GENETIC ALGORITHM

It is always a challenge to optimize the design of this special motor, both when producing or applying it as a fan drive. Since Genetic Algorithm was presented as computer algorithm, a wide range of applications appeared in various scientific areas. The main characteristic of GA program for optimization is reliable convergence and fast execution.

When using GA tool for optimization of the shaded pole motor, at the beginning a mathematical model based on the method of revolving field theory, is derived. Since target optimization function is selected to be electromagnetic torque, it is obviously that solution is maximization problem. The GA program operates under C++ programming language and creates 6000 generations of parameters' variation. In program separate input file, the range of variation of all motor variables is defined, as presented in Table I. As an output, the most favorable set of varied parameters is obtained. They are presented in Table I, too.

TABLE I Motor Parameters Variations

Motor parameter	Variation range	Output
Current density Δ [A/mm^2]	$3.5 \div 8$	5.00
Core length [mm]	$10 \div 20$	18
Magnetic induction B [T]	$0.4 \div 0.5$	0.45
Width of stator pole b_p [mm]	$10 \div 20$	12
Shading portion of stator pole	$0.2 \div 0.3$	0.2
Angle of rotor skew [$^\circ$]	$10 \div 20$	10.023

In Table II is given the comparison between parameters of the basic motor model-BMM and optimal one-OMM. In Table III the comparison between characteristics at rated loading condition, meaning slip $s_n=0.16$, for the prototype motor as well as for the optimal designed one is presented.

TABLE II Comparison of Motor Parameters

Quantity	BMM	OMM
Stator winding wire diameter[m]	$d_{Cu}=1.4 \cdot 10^{-4}$	$d_{Cu}=1.8 \cdot 10^{-4}$
Stator winding number of turns	$W=3488$	$W=2784$
Stator winding resistance [Ω]	$R_1=492.98$	$R_1=245.3$
Stator winding reactance [Ω]	$X_1=498.17$	$X_1=904.67$
Rotor cage resistance [Ω]	$R_2=457.04$	$R_2=289.89$
Rotor cage reactance [Ω]	$X_2=76.71$	$X_2=65.994$
Shading coil resistance [Ω]	$R_3=18,474$	$R_3=18,723$
Shading coil reactance [Ω]	$X_3=127.53$	$X_3=45.075$
Mutual stator-rotor reactance [Ω]	$X_{12}=2,163.3$	$X_{12}=1,970$
Mutual stator-coil reactance [Ω]	$X_{13}=175.91$	$X_{13}=154.62$

TABLE III Comparison of Motor Characteristics

Quantity	BMM	OMM
Stator winding current I_1 [A]	0.126	0.1302
Shading coil current I_3 [A]	0.0063	0.0048
Rotor cage current I_2 [A]	0.0878	0.100891
Power factor $\cos\varphi$ [/]	0.654	0.47
Input power P_1 [W]	18.11	13.47
Output power P_2 [W]	4.15	4.511
Efficiency factor η [/]	0.229	0.33
Electromagnetic torque M_{em} [Nm]	0.018075	0.019447

In Figures 2, 3 and 4 are presented comparative characteristics of motor currents $I_1=f(s)$, $I_2=f(s)$ and $I_3=f(s)$ while in Figure 5 is presented characteristic of electromagnetic torque $M_{em}=f(s)$ for basic as well as for optimised motor model, for slip $s=(0\div1)$

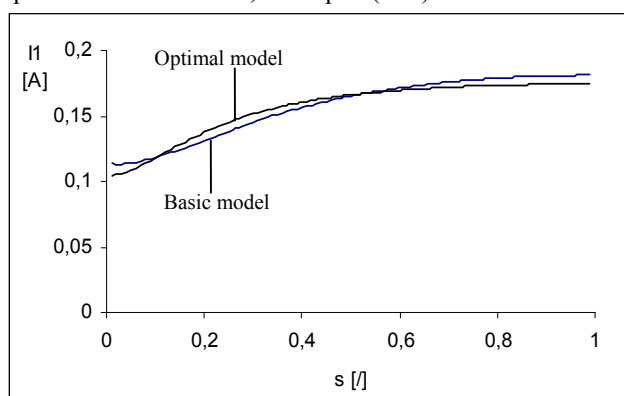


Figure 2 Characteristic of main stator winding current

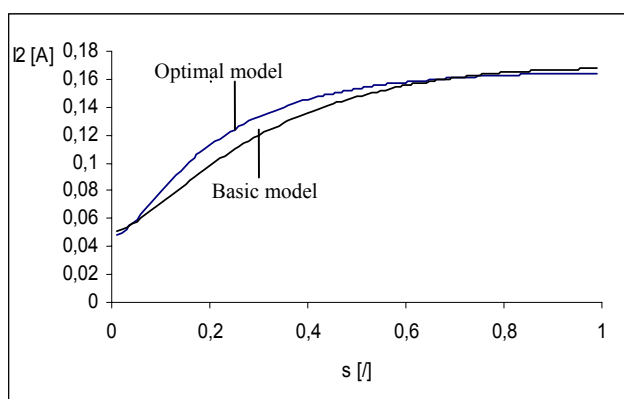


Figure 3 Characteristic of rotor cage current

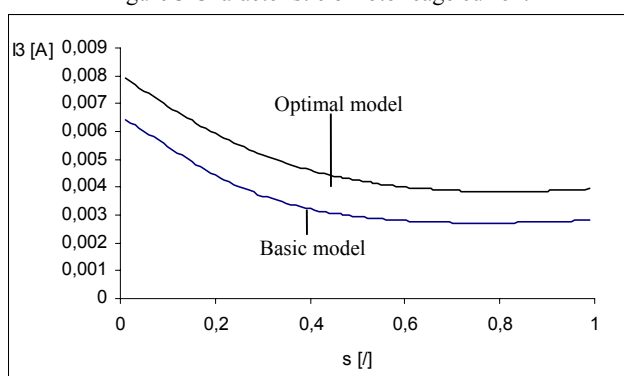


Figure 4 Characteristic of shading coil current

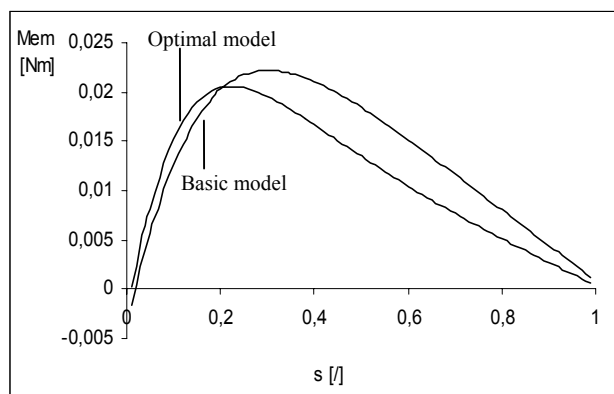


Figure 5. Characteristic of electromagnetic torque

In Figures 6, 7, and 8 are presented comparative characteristics of $P_1=f(s)$, $P_2=f(s)$ and $\eta=f(s)$ respectively.

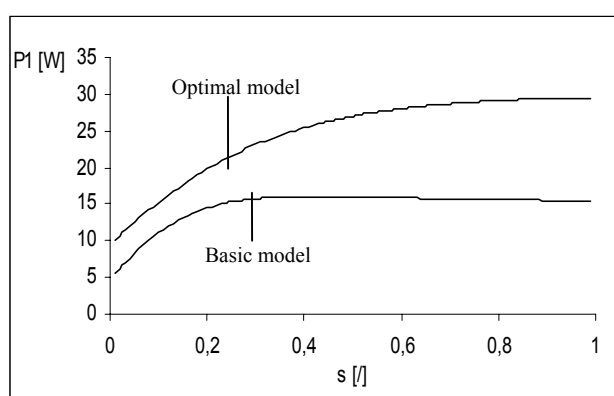


Figure 6 Characteristic of input power

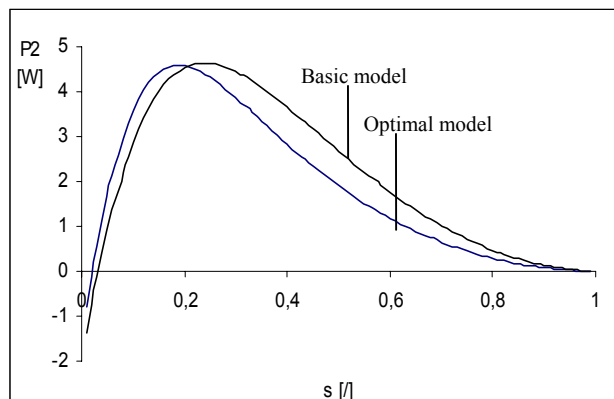


Figure 7 Characteristic of output power

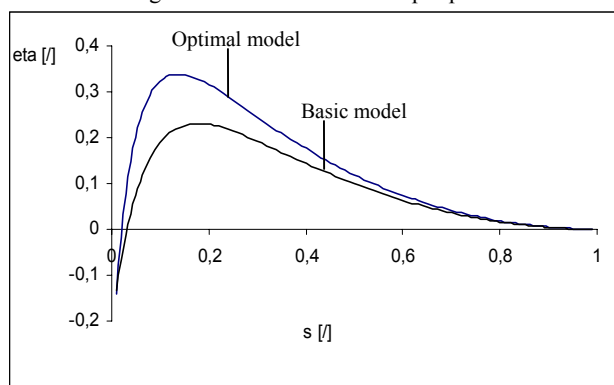


Figure 8 Characteristic of efficiency factor

From presented characteristics as well as from Tables II and III following conclusions can be drawn:

- In the optimized motor model static electromagnetic torque at rated load point is increased, mostly because of the significant increase of the excitation current in the main stator winding as it is shown in Fig.5 .

- The number of turns of the main stator winding is less for 20% in OMM leading to an increase of currents in the main stator winding, shading coil and the rotor cage winding.

- The fact that the current in the main stator winding is greater, leads to the greater values of currents in all motor windings, as is shown in Figs. 3 and 4. But apart from this fact, optimization procedure is resulting with the improved efficiency of the motor, mainly because of the significant decrease of the resistance of the windings, as presented in Table II.

- On the other hand, because of the greater diameter of the copper wire, the current density decreases effectively; this is good achievement from an operational point of view, as the motor heat losses are lower and efficiency factor is greater.

- From all relevant characteristics of the shaded-pole motor, only the power factor $\cos\phi$ in the new derived models is lower; but for this special type of motor, the gained values, as are presented in Table III, are still considered as satisfactory high.

- The angle of the rotor skewing is also changing, contributing to the reduction of the content of space field harmonics resulting in improved output torque.

IV. FINITE ELEMENT ANALYSIS

The Finite Element Method is widely used for electromagnetic field calculations in electrical machines, in general. It is usually used as a non-linear magnetostatic problem which is solved in the terms of magnetic vector potential A . However, when analysing induction machines, considering their AC excitation, the air-gap magnetic field is always a time-varying quantity. In materials with non-zero conductivity eddy currents are induced; consequently, the field problem turns to magnetodynamic, i.e. non-linear time harmonic problem. Even more, when rotor is moving, the rotor quantities are oscillating at slip frequency, quite different from the stator frequency, and the direct implementation of the non-linear time harmonic analysis is improper. The problem is solved by adjusting the rotor bars conductivity σ , corresponding to the slip. Hence, the non-linear time harmonic analysis, by using FEM, is performed at fixed stator current supply frequency $f=50\text{Hz}$, while the rotor slip is changing with load. In that case following partial equation is going to be solved numerically:

$$\nabla \times \left(\frac{1}{\mu(B)} \nabla \times A \right) = -J_{src} - \sigma \nabla V \quad (1)$$

where J_{src} represents the applied current sources. The additional voltage gradient ∇V in 2-D field problems is constant over conducting bodies. FEM considers the

equation (1) for the problems in which the field is oscillating at the single (fixed) frequency; its developed form in the 2-D domain of the motor, yields the diffusion equation for time harmonic problems which FEM is actually solving:

$$\frac{1}{\mu} \frac{\partial^2 A}{\partial x^2} + \frac{1}{\mu} \frac{\partial^2 A}{\partial y^2} = -J_{src} + j\omega\sigma A \quad (2)$$

Corresponding to the compound configuration of the motor, both in electrical and magnetic sense, and taking into consideration the particular meaning of the slip s , a motor model suitable for FEM application is derived [2]. The magnetic flux distribution in the middle cross section of prototype model and GA optimal designed model, at no load is presented in Figs. 9 and 10.

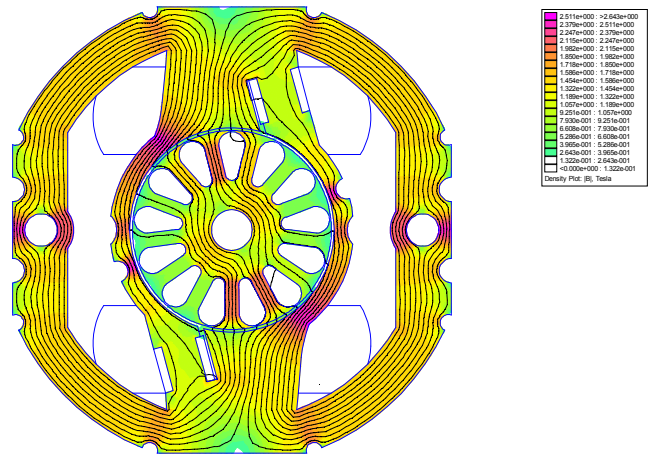


Figure 9. Magnetic flux distribution in BMM at no load

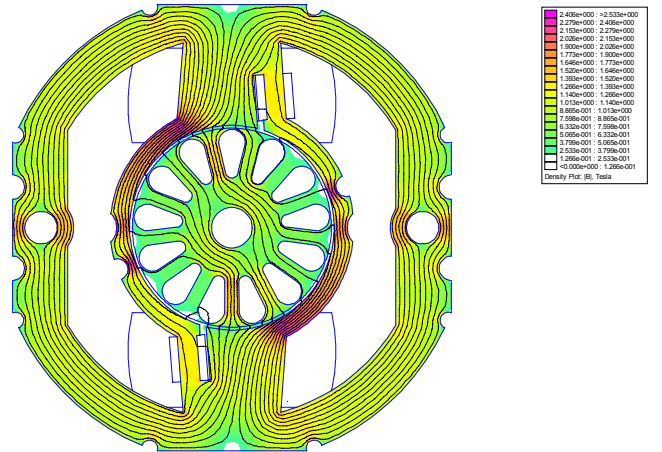


Figure 10. Magnetic flux distribution in OMM at no load

In Figs. 11 and 12 magnetic flux distribution in motor cross section at rated load is presented.

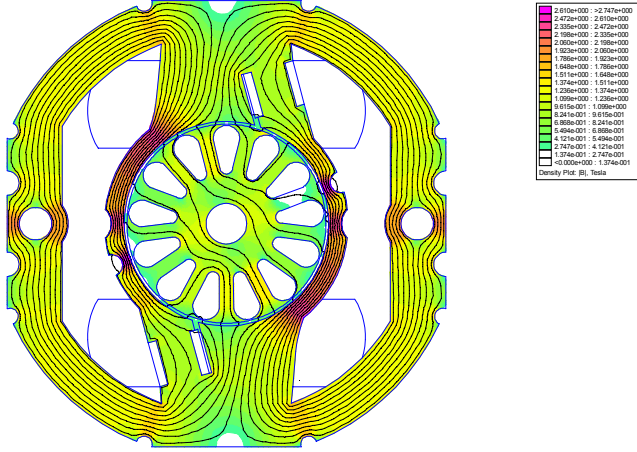


Figure.11 Magnetic flux distribution in BMM at rated load

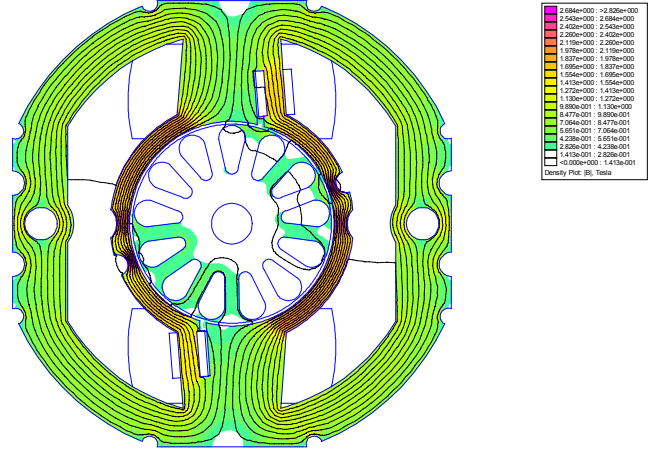


Figure.14 Magnetic flux distribution in OMM at locked rotor

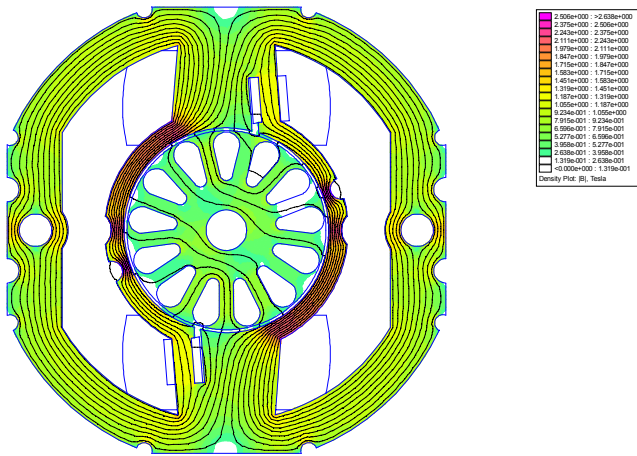


Figure.12 Magnetic flux distribution in OMM at rated load

For locked rotor position meaning slip $s=1$, magnetic flux distribution in BMM and OMM is presented in Figs. 13 and 14 respectively. From presented magnetic flux distribution in three different operating regimes can be seen that flux density in OMM is lower than in BMM. This contributes to lower iron saturation and consequently lower iron losses.

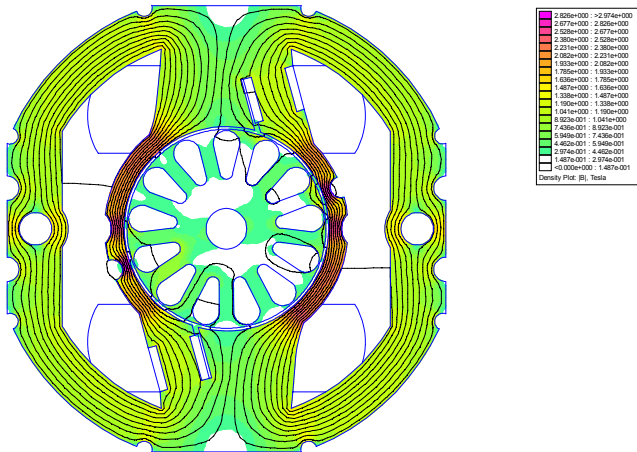


Figure 13. Magnetic flux distribution in BMM at locked rotor

V. DYNAMIC ANALYSIS

Matlab/Simulink is widely known powerful simulation tool which enables to derive and analyze motor transient performance characteristics. When simulation methods are used, the main emphasis has to be put on development of proper mathematical model, which will represent the physical phenomena as close as possible. The derived model of shaded pole motor, suitable for implementation in Matlab/Simulink is based on d,q transformation known from reference frame theory of single phase induction machines [3].

Two phase power supply is modelled using following equations:

$$\mathbf{f}_{qs} = \mathbf{K}_{2s} \mathbf{f}_{abs} \quad (3)$$

$$(\mathbf{f}_{qds})^T = [f_{as} \quad f_{ds}] \quad (4)$$

$$(\mathbf{f}_{abs})^T = [f_{as} \quad f_{bs}] \quad (5)$$

$$\mathbf{K}_{2s} = \begin{bmatrix} \cos\theta & \sin\theta \\ \sin\theta & -\cos\theta \end{bmatrix} \quad (6)$$

where: $\theta = \int \omega dt$

f represents stator and/or rotor variables.

As widely accepted transformation of single phase motor stator and rotor variables is done in stationary d,q system, meaning $\omega = 0$.

Using (3) for modeling of two phase power supply, the following equations are valid:

$$U_{qs} = U_{as} \cos\theta + U_{bs} \sin\theta \quad (7)$$

$$U_{ds} = U_{as} \sin\theta - U_{bs} \cos\theta \quad (8)$$

The specific configuration and layout of both stator windings in above equations are taken into account by introducing a phase shift between voltages. In this particular case is determined to be 43.4° .

For simulation purposes voltage equation of stator and rotor circuits are rearranged in the following form:

$$\begin{aligned}
i_{qs} &= \frac{1}{L_{lqs} + L_{mq}} \int U_{qs} - \frac{r'_{qs}}{L_{lqs} + L_{mq}} \int i_{qs} - \frac{L_{mq}}{L_{lqs} + L_{mq}} i'_{qr} \\
i'_{ds} &= \frac{1}{L'_{lds} + L_{mq}} \int U'_{ds} - \frac{r'_{ds}}{L'_{lds} + L_{mq}} \int i'_{ds} - \frac{L_{mq}}{L'_{lds} + L_{mq}} i'_{dr} \\
i'_{qr} &= \omega_r \int i'_{dr} + \frac{\omega_r L_{mq}}{L'_{lr} + L_{mq}} \int i'_{ds} - \frac{r'_r}{L'_{lr} + L_{mq}} \int i'_{qr} - \frac{L_{mq}}{L'_{lr} + L_{mq}} i_{qs} \\
i'_{dr} &= -\omega_r \int i'_{qr} - \frac{\omega_r L_{mq}}{L'_{lr} + L_{mq}} \int i_{qs} - \frac{r'_r}{L'_{lr} + L_{mq}} \int i'_{dr} - \frac{L_{mq}}{L'_{lr} + L_{mq}} i'_{ds}
\end{aligned} \quad (9)$$

In above equations r_{qs} , r'_{ds} and r'_r are resistances of main winding, shading coil and rotor winding respectively; L_{lqs} , L'_{lds} , L'_{lr} are inductances of main winding, shading coil and rotor winding; while L_{mq} is mutual inductance between stator and rotor circuits. In (9) parameters of short circuit coil and rotor winding are referred to main stator winding.

In order simulation model to be complete it is necessary to add the equation for rotor speed:

$$\frac{d\omega_r}{dt} = \frac{P^2 L_{mq}}{4J} (i'_{dr} i_{qs} - i'_{qr} i'_{ds}) - \frac{P}{2J} M_s \quad (10)$$

where: J is constant of inertia, M_s is load torque, P is number of pair of poles.

By using equations (9) and (10) transient performance characteristics of the shaded pole motor are simulated.

In Figures 15, 16 and 17, are presented the characteristics during free acceleration, as follows: speed $n_r=f(t)$, torque $M_{em}=f(t)$ and current $I_1=f(t)$, respectively; (a) is linked to the basic model and (b) to optimised motor model.

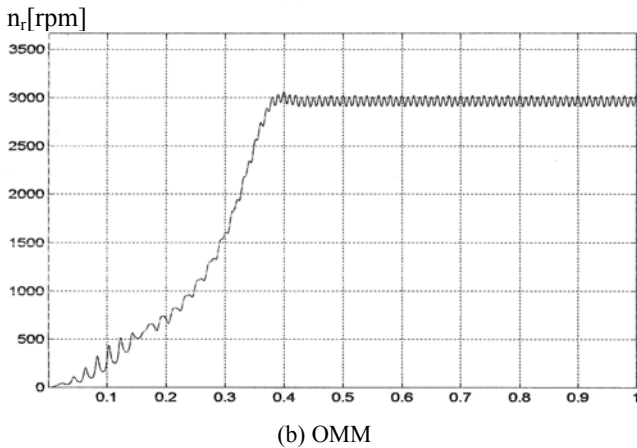
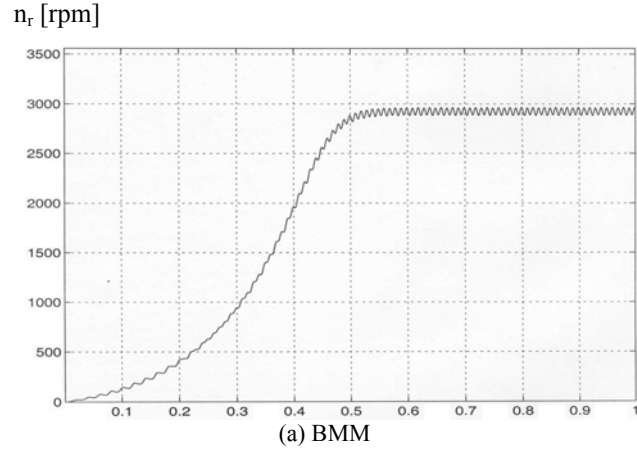


Figure 15. Rotor speed $n_r=f(t)$ at free acceleration

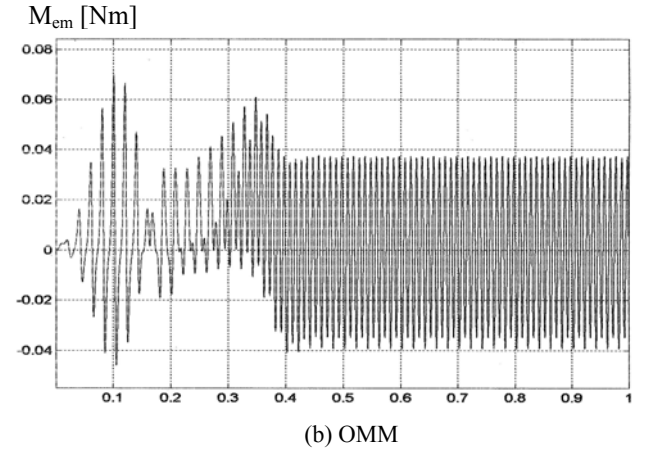
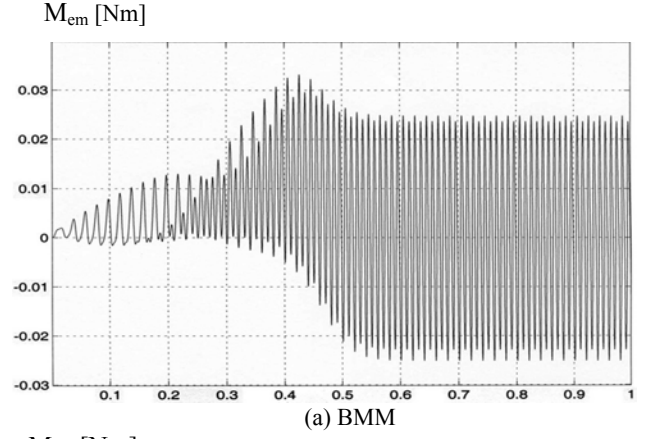


Figure 16. Torque $M_{em}=f(t)$ at free acceleration

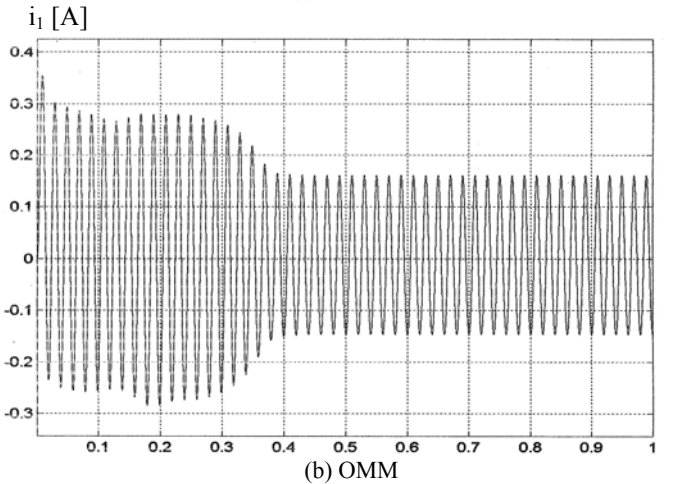
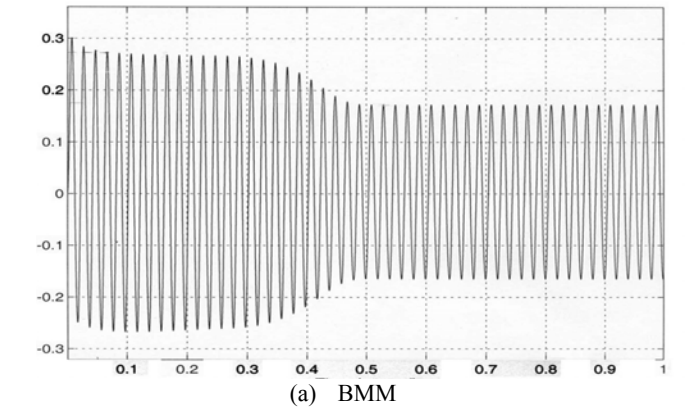


Figure 17. Main stator winding current $I_1=f(t)$ at free acceleration

Motor is assigned for fan driving, having the static torque characteristic $M_s=k \cdot n^2$; the start-up transient characteristics at rated load are presented in figures 18, 19, and 20.

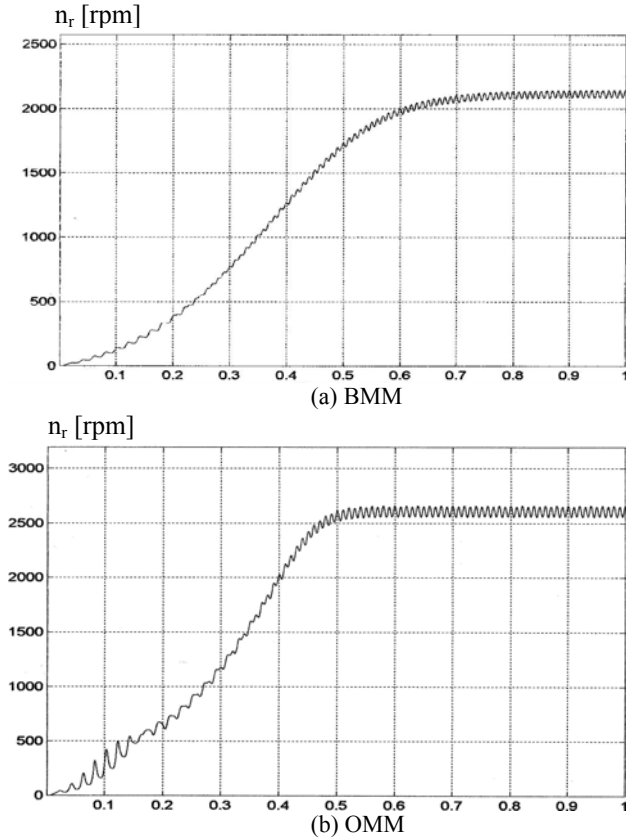


Figure 18. Rotor speed $n_r=f(t)$ at rated load

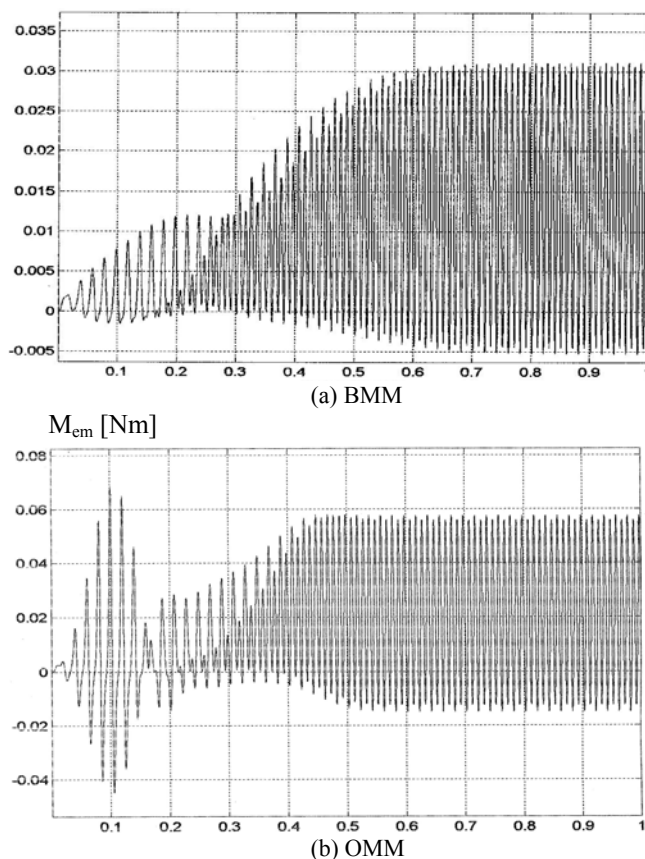


Figure 19. Torque $M_{em}=f(t)$ at rated load

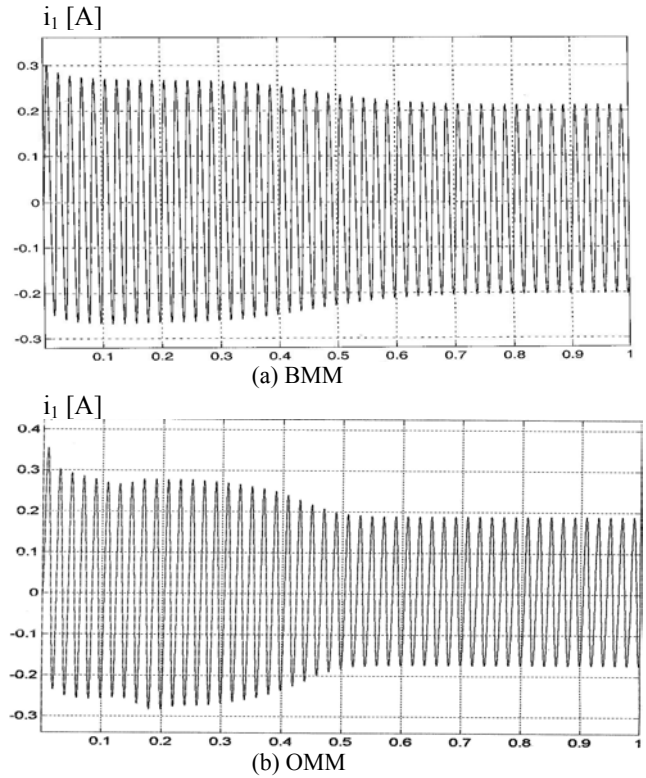


Figure 20. Main stator winding current $i_l=f(t)$ at rated load

VI. CONCLUSION

The aim of the presented work is to optimise SPM, meaning greater electromagnetic torque starting from prototype but with less constraints regarding motor cross section geometry. Using GA method is developed OMM which has 7 % larger electromagnetic torque compared to BMM. In the same time improved efficiency is achieved due to decreased resistance of main stator winding and consequently decreased copper losses. In order to analyze flux density distribution in motor cross section FEM is applied. Gained results show that in OMM at different operating regimes there is a lower flux density than in BMM, consequently lower iron saturation. FEM analysis is performed in time domain taking into consideration material non-linearity. Motor dynamic behaviour is studied using SIMULINK. From presented results it can be clearly seen that OMM has larger electromagnetic torque, due to this, shorter acceleration time, at free acceleration as well as at rated load condition. So it can be concluded that OMM is developed with better performance characteristics compared to BMM.

REFERENCES

- [1] Sarac V., Petkovska L., Cvetkovski G., "Comparison Between Two Target functions for Optimization of Single Phase Shaded Pole Motor Using Method of Genetic Algorithms", *Japanese-Mediterranean Workshop on Applied Electromagnetic Engineering for Magnetic and Superconducting Materials-JAPMED'03*, pp.43-44, 1-2 May 2003, Athens, Greece.
- [2] Sarac V., Petkovska L., Cundev M., "Non-linear Time Harmonic Analysis of Shaded-Pole Micromotor" *International Symposium on electromagnetic field Computation-ISEF'03*, vol. 1/2, pp. 137-142, 18-20 Sept. 2003, Maribor, Slovenia.
- [3] Sarac V., Petkovska L., "A Novel Approach to Performance Characteristics Evaluation of Shaded Pole Induction Motor", *Journal ELECTROMOTION*, Vol.10, No.3, pp205-210, 26-28 November 2003, Marrakesh, Morocco